

## Biosynthesis and characterisation of zinc doped iron oxide nanoparticles from *pedalium murex* and its new avenues in pharmacological applications

K.Krishnaveni<sup>1</sup>, A.S. Sakthi athithan<sup>1</sup>, J.Jeyasundari<sup>1\*</sup>,  
Y.Brightson Arul Jacob<sup>2</sup>, D.Renuga<sup>3</sup>

<sup>1,1\*</sup> (PG & Research Department of Chemistry, NMSSVN college / Madurai-625019, Tamilnadu, INDIA)

<sup>2</sup> (PG & Research Department of chemistry, The American college / Madurai -625002, Tamilnadu, INDIA)

<sup>3</sup> (PG, Department of Chemistry, Sri Meenakshi college for Women/ Madurai-625002, Tamilnadu, INDIA)

Corresponding Author: K.Krishnaveni

---

**Abstract:** Biosynthesis of metal oxide nanoparticles gains attention over the past decades due to its ecofriendly nature and provides nanoparticles with controlled size and shape. In the present work, zinc doped iron oxide nanoparticles was synthesized by co-precipitation method using *pedalium murex* leaf extract as reducing agent and capping agent. The resulting nano-particles were characterized by UV-Vis, FTIR techniques. XRD analysis shows that synthesized ZnIONPs are in hematite phase, rhombohedral in structure. The antimicrobial and anti diabetic activities of synthesized ZnIONPs are analysed by disc diffusion and pancreatic  $\alpha$ -amy method and it shows that high level of inhibition.

**Keywords:** Anti- diabetic, Anti-microbial, Co-precipitation, *Pedalium murex*, ZnIONPs

---

Date of Submission: 04-11-2018

Date of acceptance: 18-11-2018

---

### I. Introduction

Nanostructure iron oxides have attracted the attention of several researchers because of their technological utilizations such as magnetic storage media, catalysis, biomedicine, biotechnology, biosensors, etc due to their large surface area, robustness and availability [1-3]. Iron oxides can be divided into 4 types depending on their different molecular structures:  $\alpha$ -Fe<sub>2</sub>O<sub>3</sub>,  $\gamma$ -Fe<sub>2</sub>O<sub>3</sub>,  $\alpha$ -Fe<sub>3</sub>O<sub>4</sub>, and  $\gamma$ -Fe<sub>3</sub>O<sub>4</sub> [4-5]. Hematite is the most common phase of iron oxide that occurs naturally in rocks and soil. It is thermodynamically the most stable iron oxide with n-type semiconductor properties. Hematite has a complex magnetic behavior that is highly dependent on temperature and particle size. Hematite has a Néel temperature of about 948 K [6] and also undergoes a low temperature transition just below room temperature called the Morin transition [7].

Doping of transition metal ions into Fe<sub>2</sub>O<sub>3</sub> can improve the properties of nano crystalline materials by narrowing the energy-band gap and inhibiting electron-hole recombination [8]. In addition, several dopant species have been introduced into  $\alpha$ -Fe<sub>2</sub>O<sub>3</sub> in attempts to control materials properties, including Ti<sup>4+</sup>, Si<sup>4+</sup>, Nb<sup>5+</sup>, V<sup>5+</sup>, Al<sup>3+</sup>, Zn<sup>2+</sup>, and Pt<sup>4+</sup> [9]. Hence doping with transition metal impurities is a widely applied process in material science that involves incorporation of atoms or ions of appropriate elements into host lattices to yield hybrid materials with desirable properties and function. Development of new magnetic semiconductors based on the metal doped hematite is a subject of increasing research interest.

Zinc belongs to the microelements group/category that can play a vital role in many important biochemical reactions and physiological processes, such as development and growth of cells [10]. Different types of synthesis techniques are used for the synthesis of zinc-doped iron oxide nanomaterials such as bottom-up approach, viz sol-gel technique, chemical precipitation technique and in top-down, ball milling etc. Recently, great efforts were made to use green and eco-friendly method for synthesis of nanosize materials. These efforts include the use of plant or fruit extracts as surfactant [11]. The plant extracts release a variety of metabolites including carbohydrates, polysaccharides, phenols, amino acids, and vitamins, which can act as capping agents, reducing agents, stabilizing and chelating agents. The use of plant extracts in the synthesis can influence the size, the shape, and the morphology of the nanoparticles. They generate nanoparticles with high dispersity, high stability, and narrow size distribution [12-13].

The present investigation deals with the structural and magnetic characterization of zinc substituted hematite nanoparticles synthesized by co-precipitation method and it also aims to detect the anti microbial, anti diabetic activity of these nanoparticles.

## II. Materials and Methods

Plant source- leaves of *Pedalium murex*

The plant sources were collected from Sholavandan , Madurai District.

Kingdom	<i>Plantae</i>
Division	<i>Magnoliophyte</i>
Class	<i>Magnoliopsida</i>
Order	<i>Lamiales</i>
Family	<i>Pedaliaceae</i>
Genus	<i>Pedalium</i>
Species	<i>Pedalium murex</i> Linn

### 2.1 Plant description

Traditionally, *P. murex* was utilized in various ways, either as a whole plant or individual plant parts or sometimes in different special preparations. The leaves are cooked and eaten as a vegetable. In the form of powder, it can be applied locally with butter are used for rheumatic pains [14]. Leaf decoction is used to treat diabetes [15]. Leaves of *P. murex* are used to treat ulcers, dysuria, Bone fracture, diarrhea and in splenic enlargement [16]. Leaves of Alovera, *P. murex* and *Bauhinia racemosa* crushed together and mixed with water can be given to animals three times a day can relief food poisoning in cattle. An infusion or extract prepared from the different parts of the plant in cold water is used as demulcent, diuretic and also found to be best used in the treatment of disorders of urinary systems such as gonorrhoea, dysuria, incontinence of urine and vice versa[17]. The plant is also used by the local people as analgesic and antipyretic activities [18-19].



**Fig.2.1** Leaf of *Pedalium murex*

### 2.2 Chemicals required

Stock solutions of  $\text{FeCl}_3 \cdot 7\text{H}_2\text{O}$ ,  $\text{FeSO}_4 \cdot 7\text{H}_2\text{O}$  and  $\text{ZnCl}_2 \cdot 6\text{H}_2\text{O}$ ,  $\text{NH}_4\text{OH}$ .

### 2.3 Preparation of plant extract

*Pedalium murex* plant were cut into pieces and boiled with 100ml of double distilled water in a 400ml beaker for 30 minutes. The solution is then filtered through Whatman no.1 filter paper. The  $\text{p}^{\text{H}}$  value of the extract is noted. The pure filtered plant extract is stored in a container and refrigerated at  $4^{\circ}\text{C}$  for further experimental work [20].

### 2.4 Phytochemical analysis

The results for the phytochemical analysis are shown below

**Table 1.** Phytochemical analysis of the *Pedalium murex* leaf

Phytochemicals	Result
Steroid	++
Tannin	++
Flavonoid	++
Phlobatinnin	--
Terpenoids	++
Cardial glycosides	++
Reducing sugar	--



**Fig. 2.4** (a) Tests for the presence of phytochemicals in the plant extract

### **2.5 Synthesis of zinc doped iron oxide nanoparticles**

For the synthesis of these nanoparticles, co-precipitation method is employed. The standard stock solutions of  $\text{FeCl}_3 \cdot 7\text{H}_2\text{O}$ ,  $\text{FeSO}_4 \cdot 7\text{H}_2\text{O}$  and  $\text{ZnCl}_2 \cdot 6\text{H}_2\text{O}$  are added in the ratio of 2:1:1. Then the mixture is allowed to boil for 15 minutes in a magnetic stirrer with constant stirring at 460 rpm. After 15 minutes, the pure plant extract is added to the mixture and continued to boil. Then the base ( $\text{NH}_4\text{OH}$ ) is added to the mixture. The  $\text{pH}$  level is noted after each addition. The whole solution mixture is then allowed to boil for half an hour. The Nano solution is stored for UV-Vis and FTIR spectroscopic analysis.

Then the solution is centrifuged at 8000 rpm and the colloidal solution is retained. The colloidal solution obtained is then transferred to the petri plate and dried in a hot air oven at  $250^\circ\text{C}$  for 3 hours. The dried sample is again calcinated using muffle furnace.

### **2.6 Disc diffusion method**

The standardized inoculums are inoculated in the plates prepared earlier (aseptically) by dipping a sterile swab in the inoculums removing the excess of inoculums by passing, pressing and rotating the swab firmly against the side of the culture tube above the level of the liquid and finally streaking the swab all over the surface of the medium 3 times rotating the plates through an angle of  $60^\circ$  after each application. Finally pass the swab around the edge of the agar surface. Leave the inoculums to dry at room temperature with the lid closed.

The petri dish is divided into parts, in each part, sample disc such as ZnIONPs ( $100\mu\text{g}$ ) (discs are soaked overnight in sample solution) and standard Ciprofloxacin & Flucanazole ( $10\mu\text{g}$ ), are placed in the plate with the help of sterile forceps. Then petri dishes are placed in the refrigerator at  $4^\circ\text{C}$  or at room temperature for one hour for diffusion. Incubate at  $37^\circ\text{C}$  for 24 hours. Observe the zone of inhibition produced by different samples. Measure it using a scale and record the average of two diameters of each zone of inhibition.

### **2.7 Pancreatic $\alpha$ -amy assay**

The  $\alpha$ -Amy inhibitory activity of zinc doped iron oxide nanoparticles was performed, according to our former publication [21]. Briefly, amy (0.5mg/ml) was incubated with and without synthetic compounds for 10 minutes at  $25^\circ\text{C}$ . This experiment was performed in 20mM sodium phosphate buffer,  $\text{pH}$  6.9, containing 6mM sodium chloride. After pre-incubation, the starch solution was added and the reaction mixture was incubated for 30 minutes at  $25^\circ\text{C}$ . In order to stop the enzymatic reaction, dinitrosalicylic acid was added as the colour reagent and then incubated in a boiling water bath for minutes. After cooling down to the room temperature, the reaction mixture was then diluted by adding distilled water and the absorbance measured at 540 nm on a T90<sup>+</sup> UV-VIS spectrophotometer instrument [PG Instrument Ltd.,UK]. The measured absorbance was compared with that of the control experiment and the obtained result were considered as criteria for the percentage of  $\alpha$ -amy inhibition [21]. In this study, the pharmacological inhibitor, Acarbose was used as a positive control and the experiment were repeated for at least three times.

### **2.8 Uv-visible spectroscopy**

Samples [1mL] of the suspension were collected periodically to monitor the completion of bio-reduction of iron in aqueous solution, followed by dilution of the samples with 2 ml of deionized water and subsequent scan in UV-visible [vis] spectra, between wave lengths of 200 to 700 nm in a spectrophotometer [Beckman - Model No. DU - 50, Fullerton], having a resolution of 1 nm.

## 2.9 Ftir spectroscopy

FTIR analysis of the dried ZNIONPs was carried out through the potassium bromide (KBr) pellet (FTIR grade) method in 1:100 ratio and spectrum was recorded using Jasco FT/IR-6300 Fourier transform infrared spectrometer equipped with JASCO IRT-7000 Intron Infrared Microscope using transmittance mode operating at a resolution of 4 cm<sup>-1</sup>.

## 2.10 Xrd analysis

Crystallographic information about the samples was obtained from X-ray diffractometer (PANalytical, Philips PW 1830) in the range of 20°- 70° with 2°/min scanning rate, operating at 40 kV and a current of 30 mA with Cu K $\alpha$  radiation ( $\lambda = 1.5404 \text{ \AA}$ ) was used. The colloidal suspension containing metal nanoparticles was dried on a small glass slab.

## III. Results and discussion

### 3.1 Uv-visible spectroscopy

The surface Plasmon resonances (SPR) of synthesized zinc doped iron oxide nanoparticles have been studied by UV-Vis spectroscopy. After the addition of Pedalium murex leaf extract into the aqueous solution of iron chloride and iron sulphate, the solution was filled in glass cuvette of path length 10mm and UV-Vis spectral analysis has been done in the range of 300 to 700 nm. DI water was used as blank.

UV-Vis absorption spectral study may be assisted in understanding electronic structure of the optical band gap of the material. Absorption in the near ultraviolet region arises from electronic transitions associated within the sample.

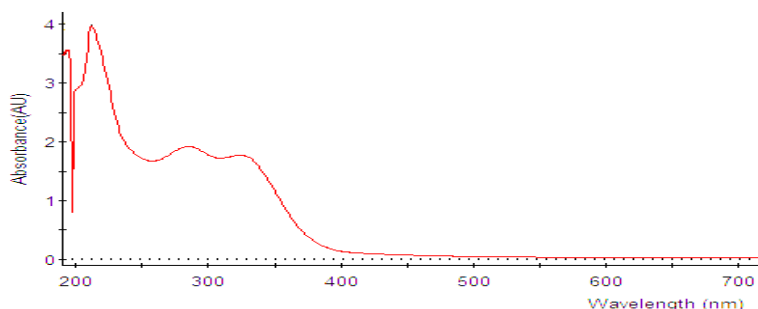


**Fig.3.1(a)** UV-Visible spectrum of plant extract (Pedalium murex)

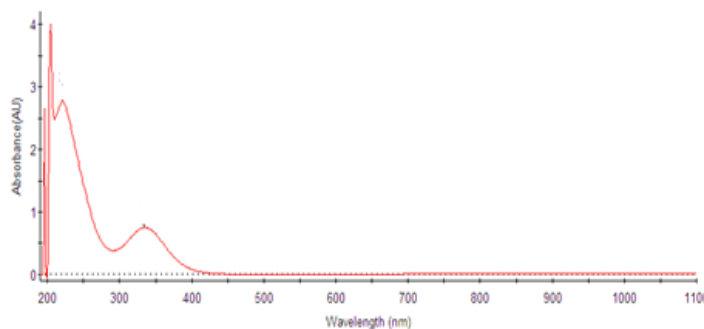


**Fig. 3.1(b)** UV-Visible spectrum for zinc doped iron oxide nanoparticles using pedalium murex.

The optical properties of synthesized iron oxide nanoparticles using UV visible spectroscopy were studied and the recorded spectra are shown in figure 3.1(a) and 3.1(b). The optical absorption of zinc doped iron oxide a nanoparticle of which is measured in a scanning range of wavelength from 300 to 800 nm.

The absorption band around at 509.25 nm by the optical absorption results [22], it is possible to determine band gap energy for the prepared sample.

### 3.1.1 Band gap calculation

The absorbance peak is related to the band gap energy, and hence using maximum absorbed wavelength, peak wavelength can be converted into band gap energy [22]. This can be converted using Einstein-plank's relation:  $E = hc / \lambda$

$$E = \frac{6.626 \times 10^{-34} \times 3 \times 10^8}{509.25}$$

$$= 2.43\text{eV}$$

The obtained band gap energy is 2.43eV and its absorption range occurs about 509.25 nm.

### 3.2 Ftir spectroscopy

The FTIR spectrum shows the presence of absorption bands associated with Fe-O stretching vibrations. These peaks represent the following bonding in the sample confirms the reducing agent role in the formation of iron oxide nanoparticles. The peak observed at  $3424\text{ cm}^{-1}$  corresponds to the -OH, -NH stretching vibrations denotes the aqueous phase as well as reduction of iron salts. The bands observed at  $1623\text{ cm}^{-1}$ ,  $1384\text{ cm}^{-1}$  are due to the C-O stretching C=O stretching mode of carbonyl functional groups in alcohol, ethers, acids and esters denotes the phytochemical present in the plant extract which stabilize as well as act as capping agent. The strong peaks at  $548\text{ cm}^{-1}$ ,  $465\text{ cm}^{-1}$  corresponds to the inorganic stretching indicates the  $\text{Fe}_2\text{O}_3$ . This suggests that biological molecule could possibly perform dual function of formation and stabilization of iron oxide nanoparticles in the aqueous medium. These results implied that tannins, saponins, flavonoids, steroids, amino acids play a major role as a capping agent or reducing agent. The intensity of absorption band at  $548\text{ cm}^{-1}$  is stronger than at  $465\text{ cm}^{-1}$ . It gives evidence for the formation of zinc doped  $\alpha\text{-Fe}_2\text{O}_3$  [23] and this is in agreement with the XRD measurement

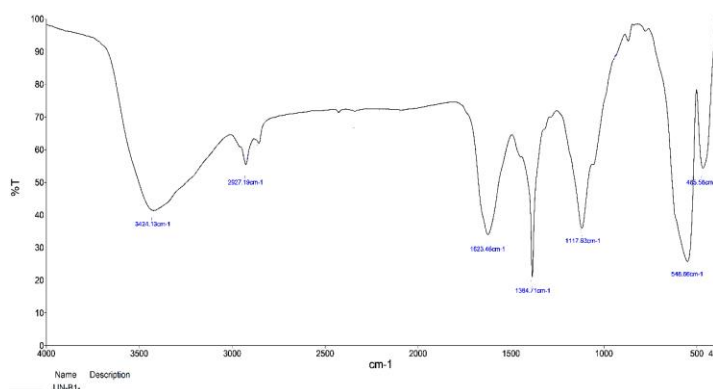


**Fig. 3.2** FTIR spectrum of zinc doped iron oxide nanoparticles

### 3.3 Xrd analysis

The XRD data is used in interpretation of grain size of crystal using Debye –Scherrer formula:

$$D = 0.9\lambda / B \cos\Theta$$

where D is the particle size

$\lambda$  is the wavelength of the incident x-ray beam

$\Theta$  is the Bragg's diffraction angle

B is full width at half maxima (FWHM) of the zinc doped iron oxide peak

The calculated size of the Nano crystallites with the Scherrer formula was 40.49 nm. The intense XRD patterns clearly showed the crystalline nature of the nanoparticles. The distinct peaks observed at 24.3150, 33.2925, 35.4381, 49.7152, 54.0576, 56.7577, 62.4739 accounting for crystal planes at (0,1,2), (1,0,4), (1,1,0), (0,2,4), (1,1,6), (2,1,1), (2,1,4) respectively. These planes represent the synthesized iron oxide nanoparticles are in hematite phase ( $\alpha\text{-Fe}_2\text{O}_3$ ), rhombohedral in structure (JCPDS file no 89-8104).

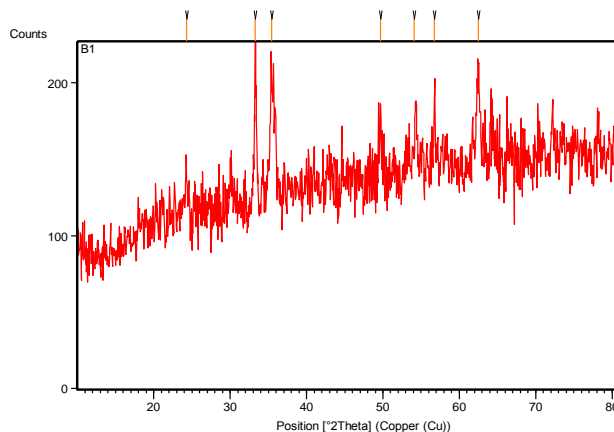


**Fig. 3.3** XRD pattern for the zinc doped iron oxide nanoparticles



### 3.4 Anti-bacterial activity

The anti-bacterial activity was tested by using disc diffusion method against two bacterial species. Among them, one is gram-positive and the other is gram negative such as Staphylococcus aureus and Escherichia coli [24].

Ciprofloxacin is kept as the standard sample and the zone of inhibition is noted.



3.4 (a)



3.4 (b)

**Fig.3.4** Inhibition zone of Escherichia coli (a) and Staphylococcus aureus (b)

**Table 2-** Antibacterial activity of ZnIONPs

Organisms	Zone of inhibition	
	Standard Ciprofloxacin [10µg/disc]	Samples [100µg/disc]
Staphylococcus aureus	32	20
Escherichia coli	48	23

### 3.5 Anti-fungal activity

The synthesized nanoparticles were tested against two fungal species i.e. Aspergillus niger and Candida albicans by disc diffusion assay [25]. Fluconazole, a commercial antifungal drug is kept as the standard sample. The zone of inhibition is noted.



3.5 (a)



3.5 (b)

**Fig.3.5** Inhibition zone of Candida albicans (a) and Aspergillus niger (b).

**Table 3-** Antifungal activity of ZnIONPs

Organisms	Zone of inhibition[mm]	
	Standard Fluconazole [10µg/disc]	Sample [100µg/disc]

Aspergillus niger	11	10
Candida albicans	10	12

### 3.6 Anti diabetic activity

#### 3.6.1 The inhibition activity of zinc doped iron oxide nanoparticles against $\alpha$ -amy

The anti-diabetic activity was tested by using pancreatic  $\alpha$ -amy assay method. Inhibition of  $\alpha$ -amy is considered a useful strategy for the treatment of disorders in carbohydrate uptake, such as diabetes and obesity as well as the dental caries and periodontal disease[2]. Acarbose, a commercial antidiabetic drug is kept as the standard sample and then inhibitory activity of zinc doped iron oxide nanoparticle is noted.

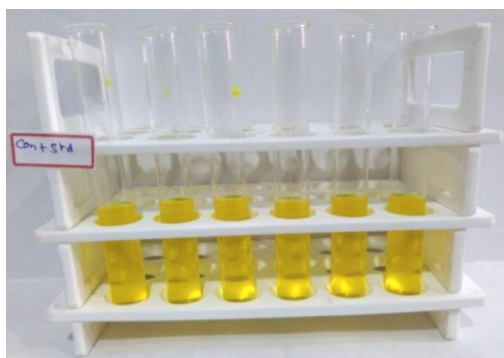


Fig. 3.6.1 (a) Inhibition zone of Acarbose



Fig 3.6.1 (b) inhibition zone of blank (plant extract)

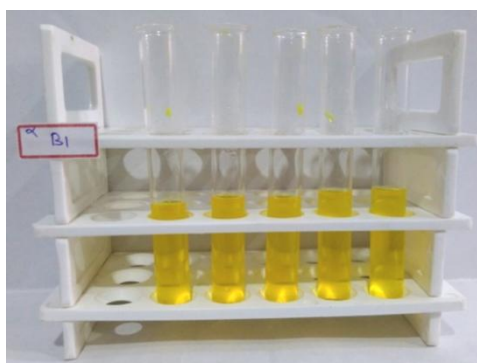


Fig. 3.6.1 (c) Inhibition zone of ZnIONPs

**Table – 4** Anti diabetic activity of ZnIONPs

Concentration	Blank	Standard [Acarbose]	ZnIONPs
20	10.12	17.68	13.46
50	15.55	29.32	23.42
100	25.76	50.42	36.56
150	42.23	65.66	60.42
200	63.33	89.98	78.87

### IV. Conclusion

The present work showed that zinc doped iron oxide nanoparticles were synthesized by co-precipitation method using *Pedalium murex* as reducing agent. In UV-Vis Analysis, the peak observed at 509.25nm shows the formation iron oxide nanoparticles and the calculated band gap energy is 2.43eV. FTIR analysis shows that the peaks observed at 548cm<sup>-1</sup> and 465cm<sup>-1</sup> concludes the formation of zinc doped iron oxide nanoparticles. XRD analysis shows that the size of synthesized nanoparticles is 40.49nm, the prepared iron oxide nanoparticles are in hematite ( $\alpha$ -Fe<sub>2</sub>O<sub>3</sub>) phase. The synthesized zinc doped iron oxide shows good antimicrobial and anti diabetic activity.

## References

- [1]. L. Machala, R. Zboril and A. Gedanken, Amorphous iron (III) oxide-A review, *Journal of Physical Chemistry B*, 111(16), 2007, 4003-4018 .
- [2]. S. Sakurai, A. Namai, K. Hashimoto and S.J. Ohkoshi, First observation of phase transformation of all four Fe<sub>2</sub>O<sub>3</sub> phases ( $\gamma$   $\epsilon$   $\beta$   $\alpha$ -phase), *Journal of the American Chemical Society*, 131(51), 2009, 18299-18303.
- [3]. N.D. Phu, D.T. Ngo, L.H. Hoang, N.H. Luong, N. Chau and N.H. Hai, Crystallization process and magnetic properties of amorphous iron oxide nanoparticles, *Journal of physics D : Applied Physics*, 44(34), 2011, 345002-345008.
- [4]. R.M. Cornell, U. Schwertmann, *The iron oxides: structure, properties, reactions, occurrences and uses* (John Wiley & Sons, 2003).
- [5]. F. Bødker, M.F Hansen, C.B. Koch, K. Lefmann, S. Mørup, Magnetic properties of hematite nanoparticles, *Physical Review B* , 61(10), 2000, 6826-6838.
- [6]. D.J Dunlop, Ö. Özdemir, *Rock magnetism fundamentals and frontiers*, (Cambridge University Press, Cambridge, 1997).
- [7]. Ö. Özdemir, D.J Dunlop, and T.S Berquó, Morin transition in hematite: size dependence and thermal hysteresis, *Geochemistry , Geophysics , Geosystems* , 9(10), 2008, 1-12.
- [8]. R. Suresh, R. Prabu, A. Vijayaraj, K. Giribabu, A. Stephen, and V. Narayanan, Facile synthesis of cobalt doped hematite nanospheres : Magnetic and Their Electrochemical Sensing Properties, *Materials Chemistry and Physics*, 134(2-3), 2012, 590-596.
- [9]. S. Cho and K.H. Lee, Synthesis of vertically aligned single-crystalline-(Fe<sub>x</sub>Cr<sub>1-x</sub>)<sub>2</sub>O<sub>3</sub> nanostructure arrays by microwave irradiation and their growth mechanism, *Crystal Engineering Communication*, 12(10), 2010, 3235–3242.
- [10]. M. X. X. C. A. S. Z. X. Hu, Room-temperature magneto resistance effects of Ag added fe<sub>3</sub>o<sub>4</sub> films with single-domain grains, *Solid State Communications*, 142(10), 2007, 595-599.
- [11]. Zahra Rezay Marand, study of magnetic and structural and optical properties of Zn doped Fe<sub>3</sub>O<sub>4</sub> nanoparticles synthesised by coprecipitation method by biomedical application, *Nanomedicine Journal*, 1(4), 2014, 238-247.
- [12]. P. Laokul, V. Amornkitbamrung, S. Seraphin, and S. Maensiri, Characterization and magnetic properties of nanocrystalline CuFe<sub>2</sub>O<sub>4</sub>, NiFe<sub>2</sub>O<sub>4</sub>, ZnFe<sub>2</sub>O<sub>4</sub> powders prepared by the Aloe vera extract solution, *Current Applied Physics*, 11(1), 2011, 101–108.
- [13]. R. S. Varma, Greener approach to nanomaterials and their sustainable applications, *Current Opinion in Chemical Engineering*, 1(2), 2012, 123–128.
- [14]. S.S. Katewa, B.L. Chaudhary, A. Jain, Folk herbal medicines from tribal area of Rajasthan, India, *Journal of Ethnopharmacology*, 92(1), 2004, 41-46.
- [15]. V. Balakrishnan, P. Prema, K.C. Ravindran, J.P Robinson, Ethnobotanical studies among villagers from dharapuram taluk, tamil nadu, india., *Global Journal of Pharmacology*, 3(1), 2009, 8-14.
- [16]. A. Jain, S.S. Katewa, B.L Chaudhary, P. Galav, Folk herbal medicines used in birth control and sexual diseases by tribals of southern Rajasthan, India., *Journal of Ethnopharmacology*, 90(1), 2004, 171-177.
- [17]. J. Leroy, Composition, origin, and affinities of the madagascan vascular flora., *Annals of the Missouri Botanical Garden*, 65(2), 1978, 535-589.
- [18]. Y.N Shukla, S.P.S. Khanuja, Chemical, pharmacological and botanical studies on Pedaliu murex, *Journal of medicinal and Aromatic Plant Sciences*, 26(1), 2004, 64-69.
- [19]. P.G Pietta , Flavonoids as antioxidants, *Journal of Natural products*, 63(7), 2000, 1035-1042.
- [20]. J. Jeyasundari et al, Green synthesis and characterization of zero valent iron nanoparticles from the leaf extract of psidium guajava plant and their antibacterial activity, *Chemical Science Review and Letters*, 6(22), 2017, 1244-1252.
- [21]. A.Yousefi et al, Novel curcumin based pyrano (2,3-d) pyrimidine antioxidant inhibitors for  $\alpha$ -amylase and  $\alpha$ -glycosidase : Implications for their pleiotropic effects, against diabetes complications , *International journal of biological macromolecules*, 78, 2015, 46-55.
- [22]. Lahure et al, Preparation and characterization of zinc doped magnetite nanoparticles using green synthesis, *International Journal of Research in chemistry and environment*, 5(4), 2015, 60-64.
- [23]. G. Wu, X. Tan, G. Li, C. Hu, "Effect of preparation method on the physical and catalytic property of nanocrystalline Fe<sub>2</sub>O<sub>3</sub>, *Journal of alloys and Compounds*, 504, 2010 , 371–376.
- [24]. A. Elumalai et al , Reviw on therapeutic uses of pedaliu murex, *International Journal of Research in Ayurveda and pharmacy*, 2(6), 2011,1743-1745.
- [25]. K. Anandalakshmi et al, Characterization of silver nanoparticles by green synthesis method using pedaliu murex leaf extract and their anti bacterial activity, *Applied Nanoscience* , 6, 2016, 399–408 .

K.Krishnaveni. " Biosynthesis and characterisation of zinc doped iron oxide nanoparticles from pedaliu murex and its new avenues in pharmacological applications. ""IOSR Journal of Pharmacy and Biological Sciences (IOSR-JPBS) 13.6 (2018): 67-74.